Transactions of the TSME (2018) Vol. 6, No. 1, 50-62
Journal of Research and Applications in Mechanical Engineering

ISSN 2229-2152 print
DOI: 10.14456/jrame.2018.6

Research Article

THERMAL PERFORMANCE AUGMENTATION IN HEAT EXCHANGER TUBE WITH OVAL–PENTAGON RINGS

W. Chingtuaythong[1]
S. Chokphoemphun[2,*]

[1]Department of Industrial Technology, Faculty of Industrial Technology, Thepsatri Rajabhat University, Lopburi, 15000, Thailand
[2]Thermal Engineering and Fluid System Research Unit (TEF), Mechanical Engineering, Faculty of Industry and Technology, Rajamangala University of Technology Isan Sakonnakhon Campus, Sakonnakhon, 47160, Thailand

ABSTRACT:
The paper presents an experimental and numerical investigation on thermal performance in a uniform wall heat-fluxed tube inserted with 45° inclined oval–pentagon rings (OPRs) for turbulent flow region using air as the working fluid. The ring parameters included three blockage ratios (R_B=e/D=0.05, 0.10 and 0.15) and four pitch ratios (R_P=P/D=1.0, 1.25, 1.5 and 2.0) are introduced. The results from the inserted tube are compared with those from smooth tube alone and show that the OPR can augment the heat transfer rate and friction loss around 2.25–4.86 and 14–100 times over the smooth tube, respectively, depending upon operating conditions. The maximum thermal enhancement factor for using OPR turbulators at about 1.36 is for Re≈3900, R_B=0.05 and R_P=1.0. It is worth noting that the results of numerical study are in good agreement with the experimental ones. The average deviation of both results is within ±7% for Nusselt number and ±10% for friction factor.

Keywords: *Thermal performance, vortex ring, flow behavior, heat tranfer, Reynolds number*

1. INTRODUCTION

The aim of enhancing heat transfer is to reduce overall sizes of the heat exchanger, possibly their cost or to reduce the energy consumption in the heat transfer process, resulting in a saving of operating costs. Therefore, many researchers have been carried out to investigate the influence of various heat transfer enhancement methods on thermal performance enhancement in a heat exchanger system both experimentally and numerically. Several investigations on thermal behaviors of using turbulators with different geometries inserted in the heat exchangers have been rich in the literature, for example, twisted/helical tapes [1–3], wire coils [4–6], baffles/ribs/winglet [7–9] and vortex ring [10–18] as shown in Table 1.

The effect of alternate axes twisted tapes with different alternate lengths to twist length ratio, l/y = 0.5, 1.0, 1.5 and 2.0 on heat transfer enhancement in a tube heat exchanger has been investigated by Eiamsa-ard et al. [1]. Chang et al. [2] examined the pressure drop coefficients and the axial heat transfer distributions of the tube inserted with a broken twisted tape with different twist ratios of 1, 1.5, 2, 2.5 or ∞. Influence of the tube fitted with the full-length helical tape with and without a centered-rod and the regularly-spaced helical tape on heat transfer enhancement was reported by Eiamsa-ard and Promvonge [3]. Keklikcioglu and Ozceyhan [4] used the triangular cross-sectioned coiled-wire mounted above the inner tube wall and the effect of relative pitches and relative triangle side length on heat transfer was reported in their study.

* Corresponding author: S. Chokphoemphun
E-mail address: chok_suriya_@hotmail.com

Table 1: Turbulators application for heat transfer enhancement in heat exchangers.

Twisted/helical tapes		
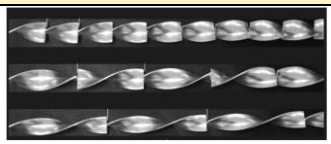		
Alternate axes twisted-tapes [1]	Broken twisted tape [2]	Regularly-spaced helical tape [3]
Wire coils		
	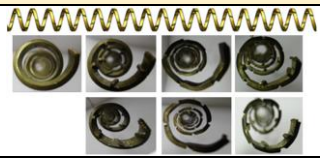	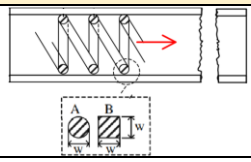
Triangle cross sectioned coiled-wire [4]	Ribbed and grooved wire coils [5]	Coiled square wires [6]
Baffles/Ribs/Winglet		
	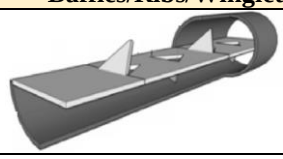	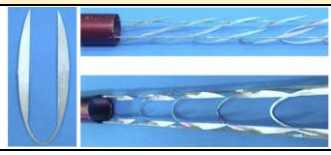
Inline winglets [7]	Delta-wing Tape [8]	Inclined horseshoe-baffles [9]
Rings turbulator		
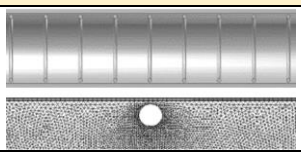	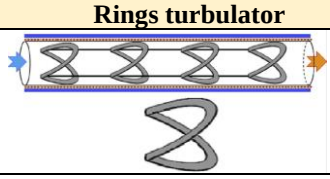	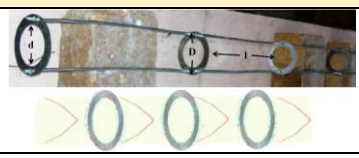
Circular rings [10]	V-shaped rings [11]	hollow circular disk [12]
	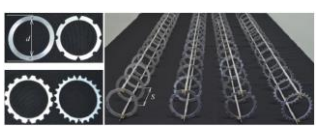	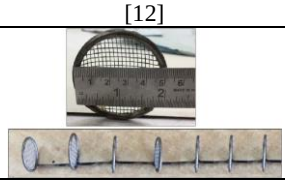
Perforated circular-ring [13]	Gear-ring [14]	Circular ring–metal wire net [15]
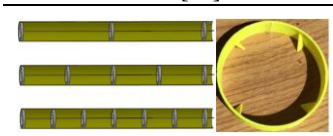	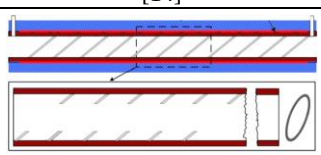	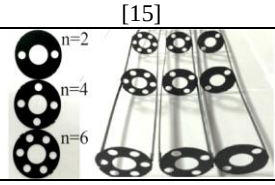
Vortex generator rings [16]	Vortex rings [17]	Circular ring [18]

Chang et al. [5] performed an experimental study on thermal performance in a tube inserted with the smooth wire coils, wire coils with 90º ribs, 90º grooves, 45º ribs, 45º grooves, 90º ribs and 90º grooves and 45º rib and 45º groove, each configuration of the wire coils came with five different pitch ratios of 0.5, 1, 1.5, 2 and 2.5. Promvonge [6] presented the effect of the coiled square wire on heat transfer, friction factor and thermal performance in a heat exchanger tube that the result was compared with the circular wire coils. Chokphoemphun et al. [7] reported the influence of winglet vortex generators (WVGs) placed in the core flow area with four different winglet pitch ratios and three blockage ratios on thermal enhancement factor of a tube heat exchanger. Eiamsa-ard and Promvonge [8] employed the double-sided delta wing tape inserted in a heat exchanger tube for heat transfer

enhancement. Promvonge et al. [9] investigated the heat transfer rate, friction factor and thermal enhancement factor in a heat exchanger tube fitted with the inclined horseshoes baffles.

The effect of circular cross-sectional rings with five different spacings between the rings was presented by Ozceyhan et al. [10]. Chingtuaythong et al. [11] examined the heat transfer and flow resistance characteristics in a round tube fitted with V-shaped rings with different relative ring-pitches and blockage ratios. Influence of the solid hollow circular disk turbulators with different diameter ratios and pitch ratios on thermal performance in a heat exchanger was reported by Kumar et al. [12]. The heat transfer and fluid friction characteristics in an air-to-water double pipe heat exchanger using perforated circular-ring were also examined by Sheikholeslami et al. [13]. Eiamsa-ard et al. [14] conducted an experimental and numerical study of friction and heat transfer behaviors in a tubular heat exchanger with gear ring turbulators. The gear rings with different free-space length ratios and tooth numbers were presented. Bartwal et al. [15] investigated the heat transfer enhancement of a tube inserted with circular ring–metal wire net with different square meshes and pitch ratios. Xu et al. [16] presented an experimental investigation on heat transfer augmentation and thermal performance in a heated tube with winglet vortex generator. Promvonge et al. [17] studied the effect of 30º inclined vortex rings with four relative ring pitches and three relative ring widths in a uniform heat-fluxed tube on thermal performance. The augmentation of heat transfer in a solar air heater using the circular ring turbulators having different hole numbers and pitch ratios was examined by Acir et al. [18].

According to the literature review above, several turbulators with various geometries have been utilized for enhancing the heat transfer rate and thermal performance in the heat exchangers. Vortex ring turbulator is one of the passive heat transfer enhancement method, which is extensively used in various heat exchangers. This is because the vortex ring can give higher heat transfer rate compared to other vortex devices such as twisted tapes or wire coils. It was apparent in the literature that the heat transfer enhancements are higher than the smooth tube in the range of 2.5–5.8, 2.7–4.5 and 1.9–4.4 times for the V-shaped rings [11], solid hollow circular disk [12] and inclined vortex rings [17], respectively. Therefore, the present research aims to employ a modified vortex-ring as a turbulence promoter for improving thermal performance of a heat exchanger. The vortex ring was designed in an oval shape with a pentagon hole drill and mounted in the test tube with attack angle of 45º with respect to the main flow direction.

2. EXPERIMENTAL SETUP

The experimental setup of a tubular heat exchanger, equipment and measuring instruments used in the present work is depicted schematically in Fig. 1. The copper tube has inner (D) and outer diameters of 50.8 and 54.8 mm, respectively and the tube was 4000-mm long, included the test section (L) of 2000-mm. The electrical wire heater was used for heating the outer tube wall of the test section during the test under a constant heat-flux condition that the electrical output power was controlled by a variac transformer. The 42 K-type thermocouples located equally on each of the top wall and the side wall were used to measure the surface temperatures along the test section while 2 RTD PT-100 thermocouples were employed to measure the inlet and outlet air temperatures at upstream and downstream of the test tube. Ceramic fiber insulation was used to prevent heat loss from electrical heater to the surrounding. A 1.5 kW blower was used for supplying ambient air into the heat exchanger tube. The flow rate of air was measured by the orifice meter, built according to ASME standard [19]. Inclined manometer was utilized for reading the pressure drop across the orifice plate and for the reference levels to adjust the airflow rate. The volumetric flow rate of air from the blower was adjusted by varying the motor speed of the blower through an inverter in the range of Reynolds number (Re) from 3900 to 20,000 covering for turbulent regime. The data logger was utilized to display and record all of the temperatures data getting from the system for calculating the heat transfer. Digital manometer was used for measuring the pressure drop across the test tube for calculating the friction factor.

A detail of the heating tube inserted with 45º inclined oval–pentagon rings (OPRs) is depicted in Fig. 2. All the OPR elements made of 2 mm thick acrylic strip having the dimension of 70-mm height by 50-mm width with a pentagon hole drill. As seen in the figure, the OPR elements with an attack angle of 45º were mounted repeatedly by using two straight steel wires to connect the rings together. The OPRs were inserted in the test section with three different winglet ring widths (e) of 2.5, 5.0 and 7.5 mm (R_B=e/D=0.05, 0.10 and 0.15) and four different pitch lengths (P) of 50, 62.5, 75 and 100 mm (R_P=P/D=1.0, 1.25, 1.5 and 2.0).

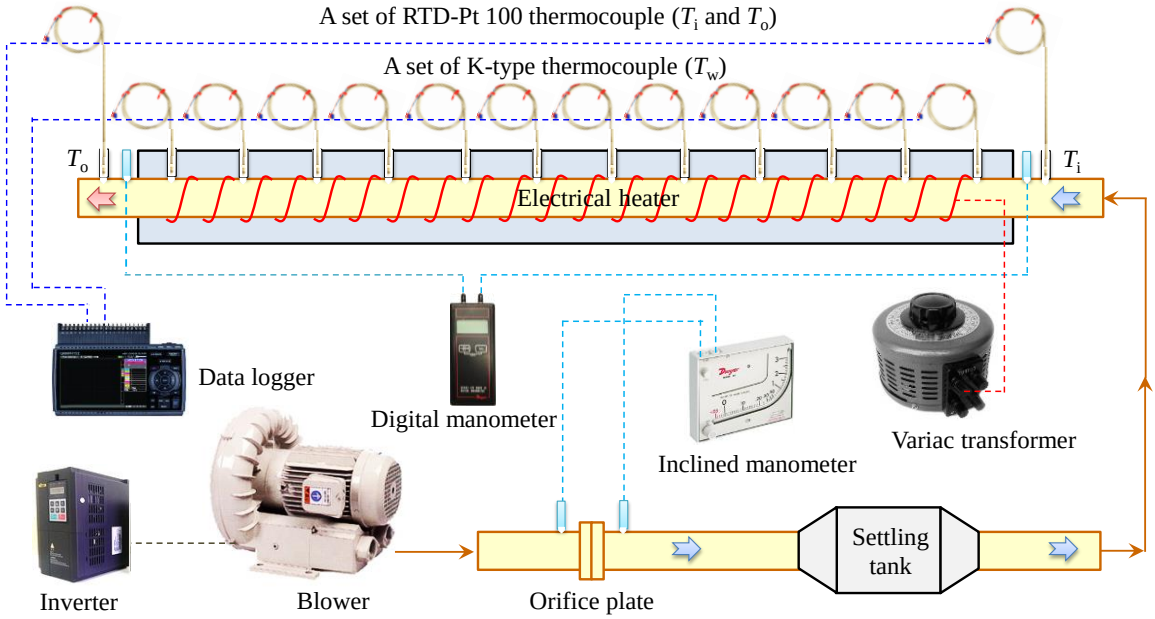

Fig. 1. Schematic diagram of the experimental setup.

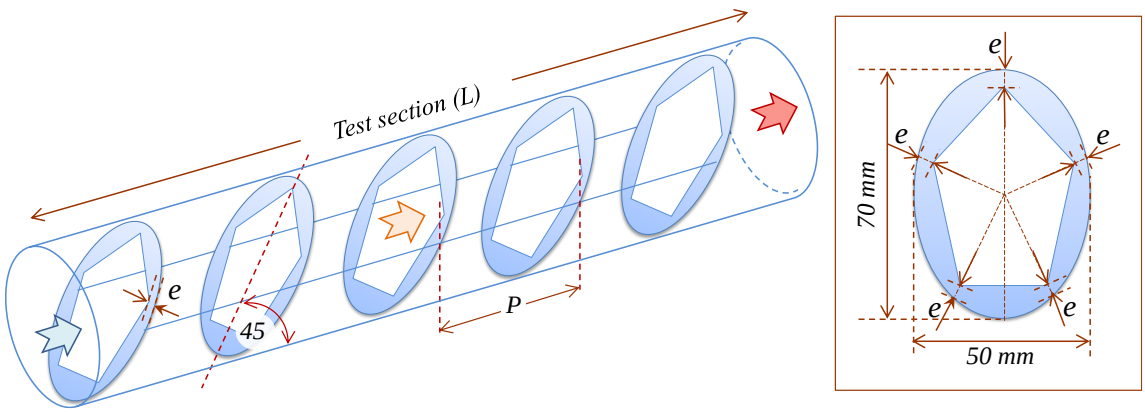

Fig. 2. Test section with inclined oval–pentagon ring (OPR) turbulator insert.

3. NUMERICAL SIMULATION

A periodic flow module and computational domain of tube inserted with OPR is depicted in Fig. 3. The heat transfer mechanism and fluid flow structure in a circular tube fitted with 45° OPRs at R_B=0.05, 0.10 and 0.15; and R_P=1.0 and 2.0, was simulated and the numerical results are validated with experimental data of the present work. The numerical study in the current work is based on the concept of periodical fully developed flow that its details have been illustrated by Patankar et al. [20]. The assumptions and governing equations of the numerical model for heat transfer and fluid flow in an inserted tube was presented in Table 2. The details of the turbulent flow model and the boundary conditions used in the present study are as shown in the reference [7]. The grid number of 250,000 cells is the appropriate both solution precision and computing time for the grid independence evaluation in the range of grid number about 60,000–500,000 cells.

Table 2: Mathematical foundation and boundary conditions.

Numerical study assumptions
Steady three-dimensional fluid flow and heat transfer
Turbulent periodic, fully developed and incompressible.
Constant air properties
Ignore body forces and viscous dissipation
Negligible radiation heat transfer
Governing equation
Continuity equation; $\frac{\partial \rho}{\partial t} + \nabla \cdot (\rho \vec{v}) = 0$
Momentum equation; $\frac{\partial (\rho \vec{v})}{\partial t} + \nabla \cdot (\rho \vec{v} \vec{v}) = \rho g - \nabla p - \nabla \cdot (\bar{\bar{\tau}})$
Energy equation; $\frac{\partial (\rho E)}{\partial t} + \nabla \cdot (\vec{v}(\rho E + p)) = \nabla \cdot \left(k_{eff} \nabla T + (\bar{\bar{\tau}}_{eff} \cdot \vec{v})\right)$

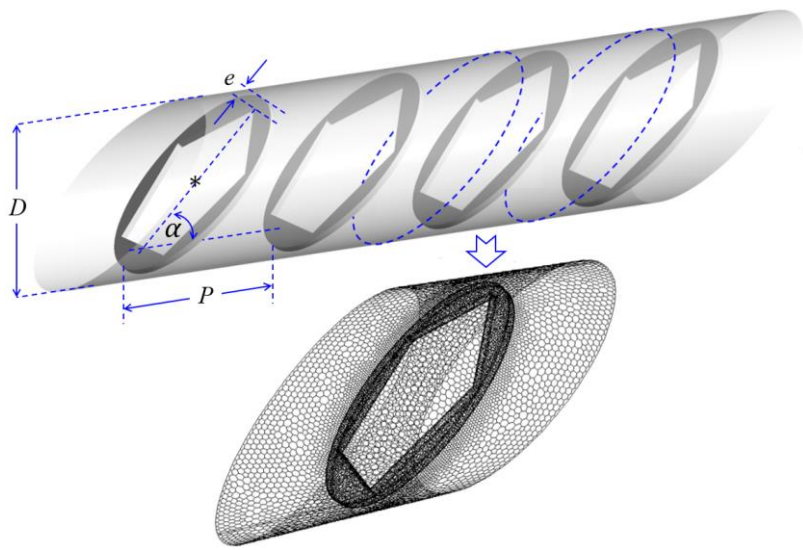

Fig. 3. Computational domain of periodic flow.

4. DATA REDUCTION

In the current work, air used as the working fluid flowed through a uniform heat-fluxed and insulated tube. The steady state convective heat transfer rate is assumed to be equal to the heat remove from the test section by working fluid.

$$\dot{Q}_{conv} = \dot{Q}_{air} \quad \rightarrow \quad hA_s(\tilde{T}_w - T_b) = \dot{m}c_p(T_o - T_i) \tag{1}$$

Therefore, the average heat transfer coefficient (h) and the Nusselt number (Nu) can be obtained by equation (2) and (3), respectively:

$$h = \frac{\dot{m}c_p(T_o - T_i)}{A_s(\tilde{T}_w - T_b)} \tag{2}$$

$$\mathrm{Nu} = \frac{hD}{k} \tag{3}$$

where $\dot{m}$ is mass flow rate, kg.s^{-1}

c_p is specific heat of air, $J.kg^{-1}.K^{-1}$
T_o is outlet temperature, K
T_i is inlet temperature, K
A_s is heat transfer surface area, m^2
$\tilde{T}_w$ is mean wall temperature, K
T_b is bulk temperature, K
h is heat transfer coefficient, $W.m^{-2}.K^{-1}$
D is inner diameter of test tube, m
k is thermal conductivity of fluid, $W.m^{-1}.K^{-1}$

The friction factor (f) computed by pressure drop across the test tube length (L) is written as

$$f = \frac{2}{(L/D)} \frac{\Delta P}{\rho U^2} \tag{4}$$

where ΔP is pressure drop, $kg.m^{-1}.s^{-2}$
L is length of test section, m
ρ is air density, $kg.m^{-3}$
U is mean air velocity, $m.s^{-1}$

In thermal performance evaluation, thermal enhancement factor (η) defined as a ratio of heat transfer coefficient for the inserted tube (h) to that of the smooth tube (h_0) at the same pumping power can be expressed as follows

$$\eta = \left.\frac{h}{h_0}\right|_{pp} = \left.\frac{\mathrm{Nu}}{\mathrm{Nu}_0}\right|_{pp} = \left(\frac{\mathrm{Nu}}{\mathrm{Nu}_0}\right)\left(\frac{f}{f_0}\right)^{-1/3} \tag{5}$$

5. RESULTS AND DISCUSSION

5.1 Test tube validation

The experimental results in terms of the Nusselt number (Nu) for heat transfer and friction factor (f) for pressure loss obtained from the present smooth tube were compared with those from correlations of Gnielinski and Petukhov, respectively, found in the literature [21] for turbulent flow in tubes as presented in Fig. 4. In the figure, the validation results are in good agreement with those from available correlations within ±8% and ±6% for Nu and f, respectively.

In addition, the heating conditions on the surface of the test tube were validated and presented in terms of the axial temperature distribution along the test section at each thermocouple location as depicted in Fig. 5. In the figure, the wall temperature displays the increasing tendency with the increment of tube lenght in the flow direction while displays a steep drop at the last two positions due to the radiation and the exit effect. This trend is similar with variation of surface temperatures along a constant surface heat-fluxed tube as described in [22].

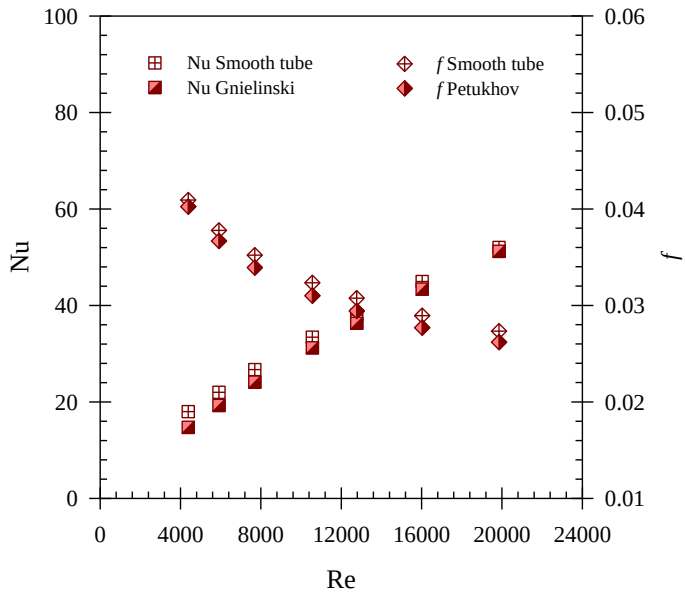

Fig. 4. Verification of Nusselt number and friction factor for smooth tube.

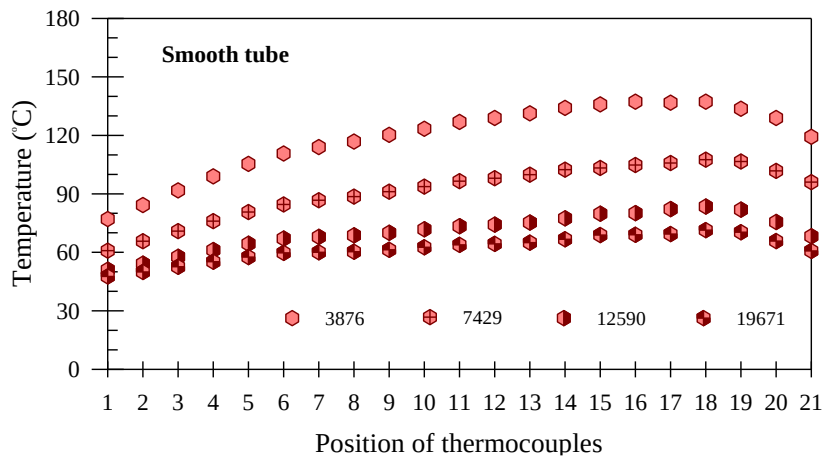

Fig. 5. Distribution of axial wall temperature the test section.

5.2 Effect of OPRs on heat transfer

The effect of 45º OPRs with various R_P and R_B values on Nu/Nu_0 plotted against Re is displayed in Fig. 6. In the figure, the OPRs yield the considerably higher heat transfer than the smooth tube alone. This is because of the flow interruption by the vortex ring turbulators resulting in the destruction of thermal boundary layer near the tube surface. The Nu/Nu_0 shows the downtrend with the increase of *Re* and R_P but with the reduction of R_B for all cases studied. For OPRs with R_P=1.0, 1.25, 1.5 and 2.0, the heat transfer values for R_B=0.05, 0.10 and 0.15 are about 2.84–3.62, 2.66–3.40, 2.54–3.24 and 2.28–2.92; 3.48–4.45, 3.17–4.06, 3.01–3.85 and 2.78–3.55; and 4.17–5.34, 3.79–4.85, 3.47–4.43 and 3.20–4.09 times above the smooth tube, respectively. At R_P=1.0, the average Nu for R_B=0.05, 0.10 and 0.15 is higher than that for R_P=1.25, 1.5 and 2.0 around 7, 12 and 24%; 10, 16 and 25%; and 10, 20 and 30% while the mean Nu for R_B=0.15 is about 17 and 42% higher than that for R_B=0.10 and 0.05, respectively.

5.3 Effect of OPRs on friction factor

Figure 7 displays the influence of 45º OPRs with different R_P and R_B values on f/f_0 plotted against *Re*, respectively. It is observed that f/f_0 tends to increase with rising *Re* for all cases. The OPRs provide the substantial increase in *f* over the smooth tube due to higher flow blockage and larger surface area inside the tube, resulting in the pressure loss increase. f/f_0 increases with decreasing R_P but rising R_B for all cases under the present experimental conditions.

At R_P=1.0, 1.25, 1.5 and 2.0, the friction loss values for R_B=0.05, 0.10 and 0.15 are about 19.12–24.88, 16.18–21.05, 14.30–18.60 and 10.97–14.27; 40.20–52.30, 33.15–43.12, 29.02–37.76 and 23.27–30.27; and 71.79–93.40, 59.82–77.83, 50.06–65.13 and 40.29–52.41 times above the smooth tube, respectively. At R_P=1.0, the mean f for R_B=0.05, 0.10 and 0.15 is higher that for R_P=1.25, 1.5 and 2.0 around 1.18, 1.34 and 1.74; 1.21, 1.39 and 1.73 and 1.20, 1.43 and 1.78 times while the mean f for R_B=0.15 is higher than that for R_B=0.10 and 0.05 at about 3.66 and 1.76 times, respectively.

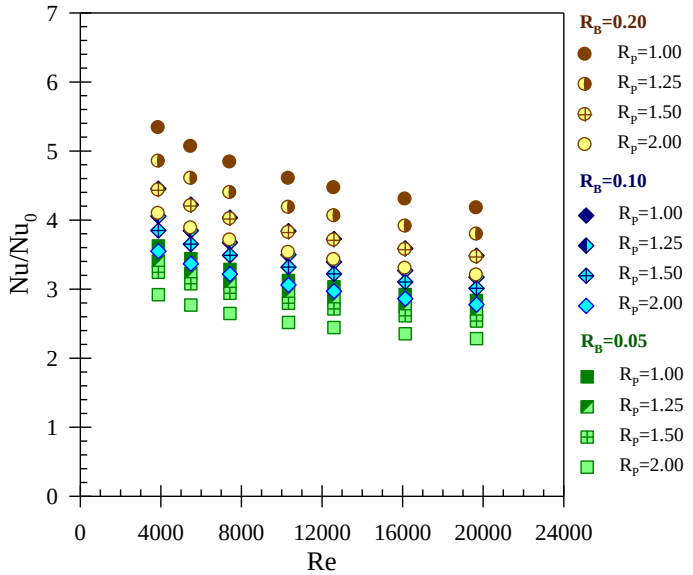

Fig. 6. Variation of Nusselt number ratio with Reynolds number for OPR insert.

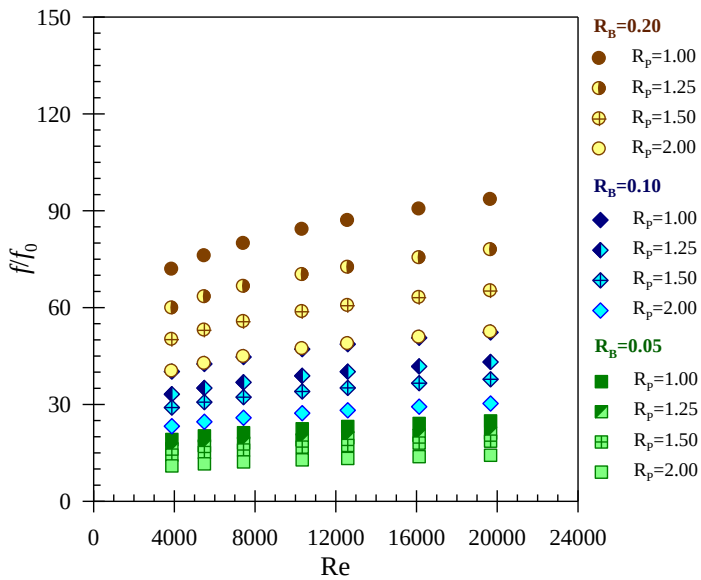

Fig. 7. Variation of friction factor ratio with Reynolds number for OPR insert.

5.4 Effect of OPRs on thermal performance

Figure 8 presents the effect of 45° OPRs with different R_P and R_B on η plotted against *Re* values. In thermal performance evaluation, the measured heat transfer and pressure loss values in each case are compared at the same pumping power condition. It is seen in the figure that η for overall range of Re is between 0.86–1.35 while for Re less than 10000, η values generally are above unity. η is found between 0.97–1.36 for R_B=0.05 and R_P=1.0 while it is 0.86–1.19 for R_B=0.15 and R_P=2.0. The highest η is found to be 1.36 at R_B=0.05 and R_P=1.0, Re≈3900. The

variations of Nusselt number ratio (Nu/Nu_0) with friction factor ratio (f/f_0) values at corresponding conditions for various R_P and R_B values are presented in Fig. 9. In the figure, it is apparent that the slope of Nu/Nu_0 with respect to f/f_0 values tends to increase with the reduction of R_B. In addition, the best performance of this work is compared with previous works is presented in Table. 3

The Nu and f correlations based on experimental data of the inserted tube were developed by relating Re, R_B and R_P and can be written as in equation (6) and (7), respectively. The errors of empirical correlations are within ±6% for Nu and ±8% for f.

$$Nu = 0.7443Re^{0.6488}Pr^{0.4}(R_B)^{0.3115}(R_P)^{-0.34} \quad (6)$$

$$f = 51.7362Re^{-0.088}(R_B)^{1.1662}(R_P)^{-0.8075} \quad (7)$$

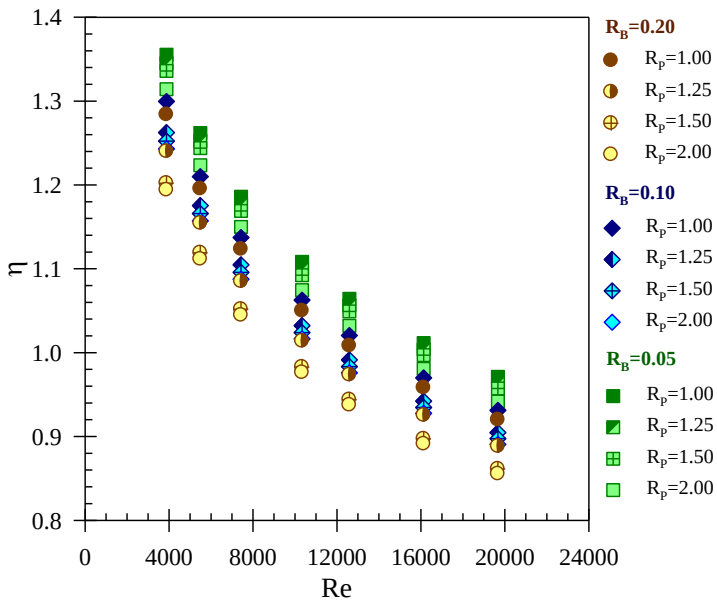

Fig. 8. Variation of thermal performance with Reynolds number for OPRs insert.

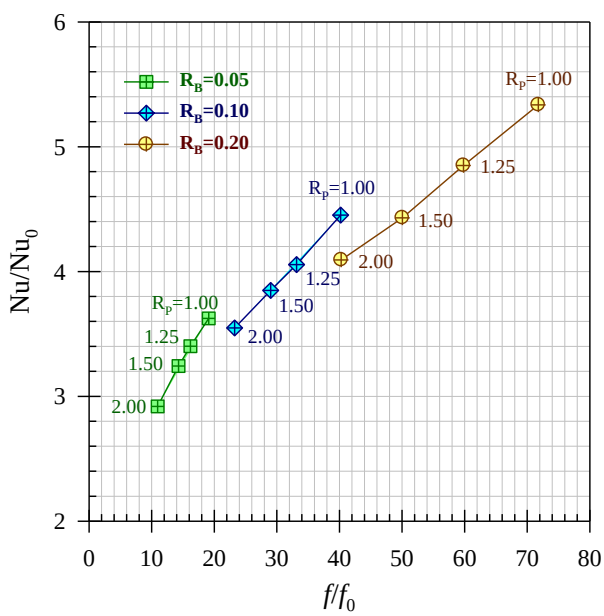

Fig. 9. Nu/Nu_0 against friction f/f_0 for various R_B and R_P.

5.5 Numerical results

The numerical results of heat transfer and pressure loss in the inserted tube with 45º OPRs are validated by comparison with experimental results under similar operating conditions as presented in Figs. 10 and 11, respectively. It is worth noting that the results of numerical study are in good agreement with experimental data. The average deviations are within ±7% for Nusselt number and ±10% for friction factor. Streamlines of impinging jet for 45º OPRs insert at Re=4000, R_B=0.05 and R_P=1.0 are depicted in Fig. 12. It is visible in the figure that there are vortex flows appear along the tube. Figs. 13 and 14 display the local Nusselt number and pressure coefficient contours for 45º OPRs insert at Re=4000, R_B=0.05 and R_P=1.0, respectively. It is apparent that the area around the OPRs displays higher local Nu values, except for the top edge of the rings. On the other hand, the surface around the tube behind the ring gives a negative pressure coefficient, as a result, the air flow is induced to impinge on this region. While in the upper surface area of the tube, upstream of the ring there is a high-pressure region and thus, results in high pressure coefficients because it is impassable for flow.

Table 3: Comparison of thermal performance for various ring turbulators.

Authors	Conditions of investigation	η_{max}
[10]	The circular cross-sectional rings with relative ring pitches of 3D and Re≈15,600	1.18
[11]	The V-shaped rings with R_B=0.1, R_P=1.0 and Re≈5000	1.63
[12]	The solid hollow circular disk diameter with ratio of 0.8, R_P=1.0 and Re≈6000	1.40
[13]	The perforated circular-ring with number of perforated hole of 8, pitch ratio of 1.83 and Re≈6000	1.17
[14]	The gear-ring elements with free space length ratio of 3.0, and tooth number of 24 and Re≈6000	1.30
[15]	The circular ring metal wire net with wire net grade of 9, pitch ratio of 3 and Re≈3,5000	2.84
[16]	The vortex generator rings with blockage ratio of 0.1, pitch ratio of 2.4, attack angle of 0º and Re≈6000	1.45
[17]	The vortex rings with relative ring width ratio of 0.1, relative ring width ratio of 0.5 and Re≈5000	1.40
[18]	The circular ring turbulators with hole number of 2, pitch ratio of 2.0 and Re≈3000	1.83
This work	The 45º inclined oval–pentagon rings turbulator with blockage ratio of 0.05, pitch ratio of 1.0 and Re≈3900	1.36

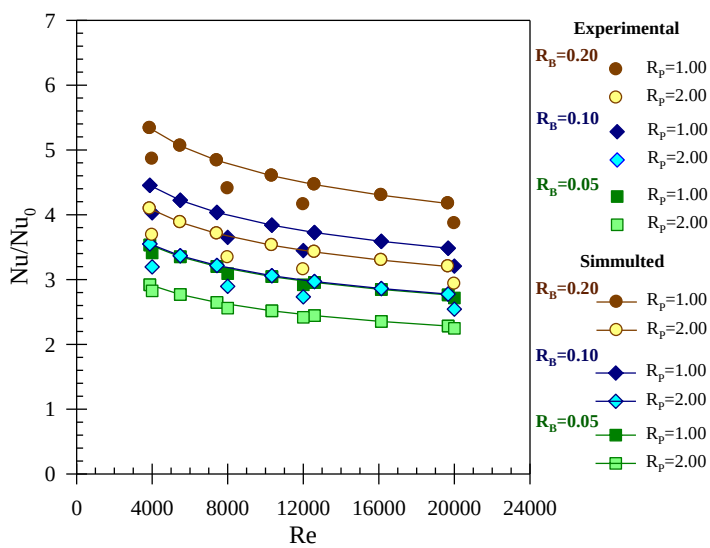

Fig. 10. Comparison between experimental and predicted Nu/Nu_0 values.

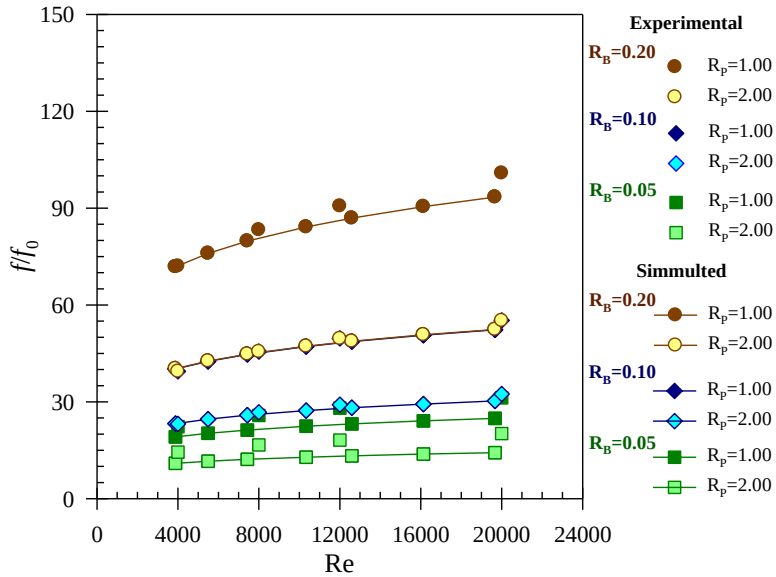

Fig. 11. Comparison between experimental and predicted f/f_0 values.

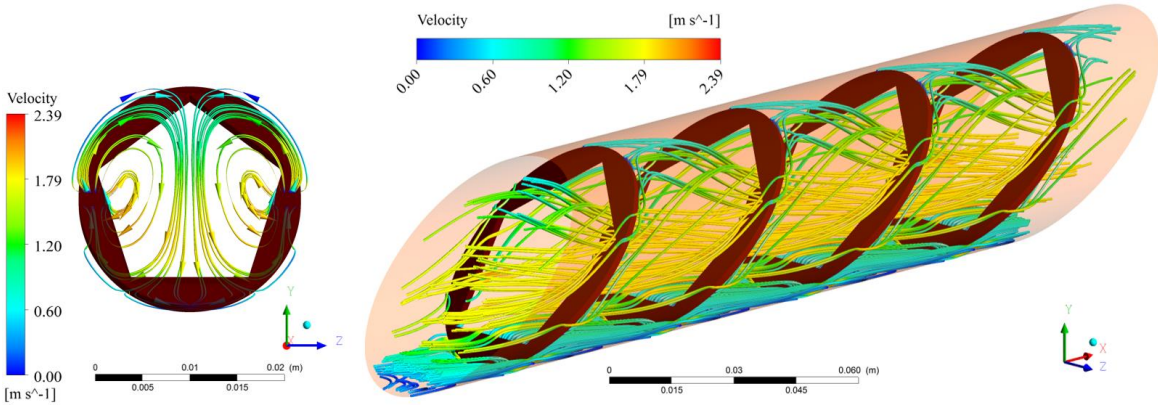

Fig. 12. Streamlines of impinging jet for 45º OPR insert at Re=4000, R_B=0.05 and R_P=1.0.

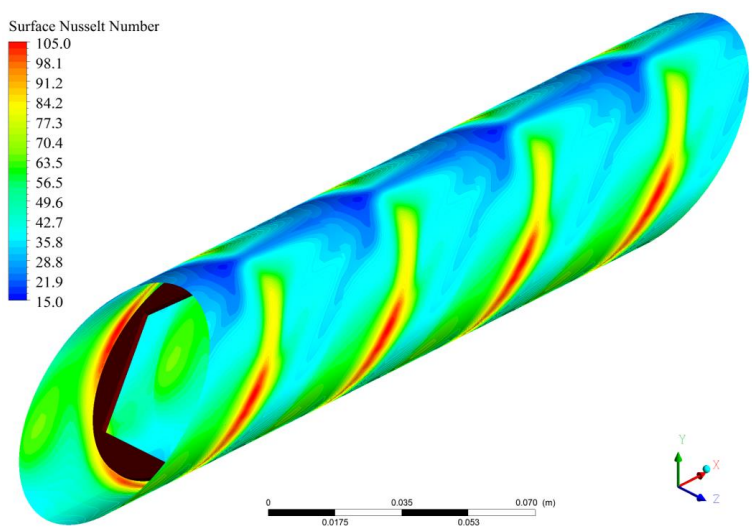

Fig. 13. Local Nusselt number contours for OPR insert at Re=4000, R_B=0.05 and R_P=1.0.

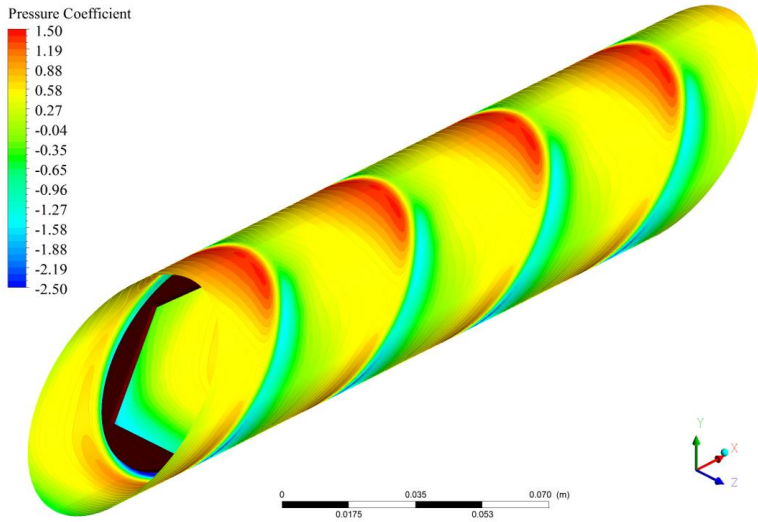

Fig. 14. Pressure coefficient contours for OPR insert at Re=4000, R_B=0.05 and R_P=1.0.

6. CONCLUSION

An experimental and numerical investigation has been performed to study the air flow friction and heat transfer characteristics in a tube inserted with 45º inclined oval–pentagon rings turbulator (OPRs) for turbulent regime under uniform heat-flux condition. The results of the present experimental study can be concluded that the heat transfer and the pressure loss increase with the rise of R_B but with decreasing R_P. The tube inserted with OPRs yields the heat transfer rate and pressure loss around 2.25–4.86 and 14–100 times above the smooth tube, respectively, depending upon operating conditions. The thermal enhancement factor decreases with the increase of R_B and R_P. The maximum thermal enhancement factor for using OPR turbulators is 1.36 at Re≈3900, R_B=0.05 and R_P=1.0 in the present work.

ACKNOWLEDGEMENT

The authors would like to gratefully acknowledge Rajamangala University of Technology Isan Sakonnakhon campus, Thai-Nichi Institute of Technology (Dr. Sombat Tamna) for support in the numerical software and finally, the Thailand Research Fund (TRF).

REFERENCES

[1] Eiamsa-ard, S., Somkleang, P., Nuntadusit, C. and Thianpong C. Heat transfer enhancement in tube by inserting uniform/non-uniform twisted-tapes with alternate axes: Effect of rotated-axis length, Appl. Therm. Eng., Vol. 54, 2013, pp. 289–309.

[2] Chang, S.W., Yang, T.L. and Liou, J.S. Heat transfer and pressure drop in tube with broken twisted tape insert, Exp. Therm. Fluid Sci., Vol. 32, 2007, pp. 489–501.

[3] Eiamsa-ard, S. and Promvonge, P. Enhancement of heat transfer in a tube with regularly-spaced helical tape swirl generators, Sol. Energy, Vol. 78, 2005, pp. 483–494.

[4] Keklikcioglu, O. and Ozceyhan, V. Experimental investigation on heat transfer enhancement in a circular tube with equilateral triangle cross sectioned coiled-wire inserts, Appl. Therm. Eng., Vol. 131, 2018, pp. 686–695.

[5] Chang, S.W., Jing Yan Gao, J.Y. and Shih H.L. Thermal performances of turbulent tubular flows enhanced by ribbed and grooved wire coils, Int. J. Heat Mass Transfer, Vol. 90, 2015, pp. 1109–1124.

[6] Promvonge, P. Thermal performance in circular tube fitted with coiled square wires, Energy Convers. Manage., Vol. 49, 2008, pp. 980–987.

[7] Chokphoemphun, S., Pimsarn, M., Thianpong, C. and Promvonge, P. Heat transfer augmentation in a circular tube with winglet vortex generators, Chin. J. Chem. Eng., Vol. 23, 2015, pp. 605–614.

[8] Eiamsa-ard, S. and Promvonge, P. Influence of double-sided delta-wing tape insert with alternate-axes on flow and heat transfer characteristics in a heat exchanger tube, Chin. J. Chem. Eng., Vol. 19(3), 2011, pp. 410–423.

[9] Promvonge, P., Tamna, S., Pimsarn, M. and Thianpong, C. Thermal characterization in a circular tube fitted with inclined horseshoe baffles, Appl. Therm. Eng., Vol. 75, 2015, pp. 1147–1155.
[10] Ozceyhan, V., Gunes, S., Buyukalaca, O. and Altuntop, N., Heat transfer enhancement in a tube using circular cross sectional rings separated from wall, Appl. Energ., Vol. 85, 2008, pp. 988–1001.
[11] Chingtuaythong, W., Promvonge, P., Thianpong, C. and Pimsarn, M. Heat transfer characterization in a tubular heat exchanger with V-shaped rings, Appl. Therm. Eng., Vol. 110, 2017, pp. 1164–1171.
[12] Kumar, A., Sunil Chamoli, S. and Kumar, M. Experimental investigation on thermal performance and fluid flow characteristics in heat exchanger tube with solid hollow circular disk inserts, Appl. Therm. Eng., Vol. 100, 2016, pp. 227–236.
[13] Sheikholeslami, M., Gorji-Bandpy, M. and Ganji, D.D. Experimental study on turbulent flow and heat transfer in an air to water heat exchanger using perforated circular-ring, Exp. Therm. Fluid Sci., Vol. 70, 2016, pp. 185–195.
[14] Ruengpayungsak, K., Wongcharee, K., Thianpong, C., Pimsarn, M., Chuwattanakul, V. and Eiamsa-ard, S. Heat transfer evaluation of turbulent flows through gear-ring elements, Appl. Therm. Eng., Vol. 123, 2017, pp. 991–1005.
[15] Bartwal, A., Gautam, A., Kumar, M., Mangrulkar, C.K. and Chamoli, S. Thermal performance intensification of a circular heat exchanger tube integrated with compound circular ring–metal wire net inserts, Chem. Eng. Process., Vol. 124, 2018, pp. 50–70.
[16] Xu, Y., Islam, M.D. and Kharoua, N. Experimental study of thermal performance and flow behaviour with winglet vortex generators in a circular tube, Appl. Therm. Eng., Vol. 135, 2018, pp. 257–268.
[17] Promvonge, P., Koolnapadol, N., Pimsarn, M. and Thianpong, C. Thermal performance enhancement in a heat exchanger tube fitted with inclined vortex rings, Appl. Therm. Eng., Vol. 62, 2014, pp. 285–292.
[18] Acir, A., Ismail Ata, I. and Canli, M.E. Investigation of effect of the circular ring turbulators on heat transfer augmentation and fluid flow characteristic of solar air heater, Exp. Therm. Fluid Sci., Vol. 77, 2016, pp. 45–54.
[19] ASME. Standard measurement of fluid flow in pipes using orifice, nozzle and venture, ASME MFC–3M-1984, 1984, ASME, New York.
[20] Patankar, S.V., Liu, C.H. and Sparrow, E.M. Fully developed flow and heat transfer in ducts having streamwise-periodic variations of cross-sectional area, ASME J. Heat Transf., Vol. 98, 1998, pp. 1109–1151.
[21] Incropera, F.P., Witt, P.D., Bergman, T.L. and Lavine, A.S. Fundamentals of heat and mass transfer, 2006, John-Wiley & Sons, New York.
[22] Cengel, Y.A. and Ghajar, A.J. Heat transfer and mass transfer fundamentals & applications, 2015, McGraw–Hill Education, New York.